



## ORIGINAL ARTICLE

# Ionic liquids functionalized $\beta$ -cyclodextrin polymer for separation/analysis of magnolol



Nan Zhou, Xia-Shi Zhu\*

College of Chemistry &amp; Chemical Engineering, Yangzhou University, Yangzhou 225002, China

Received 18 July 2013; accepted 19 December 2013

Available online 28 December 2013

**KEYWORDS**

Magnolol;  
 Ionic liquids  
 functionalized- $\beta$ -  
 cyclodextrin polymer;  
 Solid-phase extraction;  
 High-performance liquid  
 chromatography

**Abstract** Ionic liquids functionalized  $\beta$ -cyclodextrin polymer, a mono-6-deoxy-6-(1,2-dimethylimidazolium)- $\beta$ -cyclodextrin iodide polymer (ILs- $\beta$ -CDCP), was synthesized as a solid-phase adsorbent coupled with high-performance liquid chromatography for separating or analyzing magnolol in drug samples. The results showed that magnolol was adsorbed rapidly on ILs- $\beta$ -CDCP and eluted with methanol. Under the optimum conditions, pre-concentration factor of the proposed method was 12. The linear range, limit of detection (LOD), correlation coefficient ( $R$ ) and relative standard deviation (RSD) were found to be 0.02–8.00  $\mu\text{g/mL}$ , 1.9 ng/mL, 0.9992 and 2.76% ( $n=3$ ,  $c=2.00$   $\mu\text{g/mL}$ ), respectively. The interaction between ILs- $\beta$ -CDCP and magnolol was studied through the inclusion constant, FTIR and TGA analysis. This proposed method has been successfully applied to the determination of magnolol in real samples.

© 2014 Xi'an Jiaotong University. Production and hosting by Elsevier B.V.

Open access under [CC BY-NC-ND license](https://creativecommons.org/licenses/by-nc-nd/4.0/).**1. Introduction**

Solid-phase extraction (SPE) has the advantages of high enrichment factor and good selectivity. It is also characterized by easy operation, low organic solvent consumption, and little environmental pollution [1]. The selection of SPE material (solid-phase adsorbent) is one of the important factors, which

mainly include fiber [2], silica gel [3], chelating resin [4], nano material [5], active carbon [6] and cyclodextrin cross-linking polymer (CDCP) [7]. As a solid-phase extraction material, CDCP is widely used in separation/analysis of metal elements [8–10] and organic compounds [11,12]. Functionalized cyclodextrin has already become a new hotspot in supramolecular field [13]. Functionalization of cyclodextrins (CDs) can alter their physical properties and also make them suitable for a wide range of applications [14–16]. Various applications of functionalized cyclodextrins have been reported: biological-based chitosan grafted  $\beta$ -cyclodextrin for the removal of benzoic acid [14];  $\text{Fe}_3\text{O}_4$ /cyclodextrin polymer nanocomposites for the removal of heavy metals [15] and  $\beta$ -CD/ $\text{Fe}_3\text{O}_4$  modified glassy carbon electrode in tryptophan analysis [16].

Non-volatility and nonflammability are common characteristics of ionic liquids, giving them an advantageous edge in various

\*Corresponding author. Tel./fax: +86 514 7975244.

E-mail addresses: [xszhu@yzu.edu.cn](mailto:xszhu@yzu.edu.cn), [zhuxiashi@sina.com](mailto:zhuxiashi@sina.com) (X.-S. Zhu).

Peer review under responsibility of Xi'an Jiaotong University.



applications [17]. This common advantage, when considered with the possibility of tuning the chemical and physical properties of ILs by changing anion–cation combination, is a great opportunity to obtain task-specific ILs for a multitude of specific applications [18]. Interestingly, because of their high solubility power, cyclodextrins and their derivatives can be dissolved in the RTIL-stationary phases to provide additional selectivity and resolution for separations that are otherwise impossible [19]. The inclusion interaction between  $\beta$ -CD and IL surfactant 1-dodecyl-3-methylimidazolium hexafluorophosphate was reported by Li et al. [20]. The applications of ionic liquid functionalized cyclodextrins for separation/analysis include HPLC – chiral stationary phases [21]; sewage treatment – adsorbent of organic pollutants and heavy metals [22]. However, ionic liquids functionalized  $\beta$ -cyclodextrin polymer as a solid-phase extraction adsorbent for the determination of analyte in real samples seems to be lacking.

Magnolol (Fig. 1) is one of the major bioactive components of the extracts from the bark of *Magnolia officinalis*. It has an obvious and lasting inhibitory effect on the central nervous system. It is also often used in the treatment of acute enteritis, amebic dysentery, and chronic gastritis [23]. Recent research suggests that it may be a potential therapeutic for neurodegenerative disease, early granulocyte leukemia, and atherosclerosis [24]. Various methods have been developed for the determination of magnolol to date, including gas chromatography [25], supercritical fluid extraction coupled with capillary gas chromatography [26], liquid phase microextraction coupled with high-performance liquid chromatography (HPLC) [27] and fluorescence spectrometry [28–30], ultraviolet spectroscopy [31], and liquid–liquid microextraction coupled with HPLC [32]. In this work, SPE–HPLC was applied to determine magnolol. Compared with other methods, the proposed method has the advantages of quick and easy separation and preconcentration of analyte in samples.

## 2. Experimental

### 2.1. Materials and reagents

Centrifuge (Anke Scientific Instrument Factory, Shanghai, China), timing multifunctional oscillator (Guohua Co., Ltd., Changzhou, China), digital constant temperature water-bath (Guohua Co., Ltd., Changzhou, China) and PHS-25 meter (Shanghai Jinjke Co., Ltd., Shanghai, China) were used for the study.

Fourier transform infrared spectroscopy (FTIR) was measured with a Bruker Tensor27 spectrometer (Bruker Company, Germany). Samples were pressed into KBr pellets and recorded at the frequencies from 4000 to 400  $\text{cm}^{-1}$  with a resolution of 4  $\text{cm}^{-1}$ . Cross-polarization/magic angle spinning nuclear magnetic resonance (CP/MAS NMR) (Bruker Company, Germany) spectrum

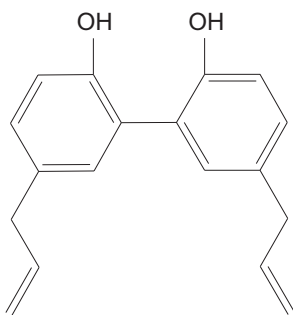


Fig. 1 The chemical structure of magnolol.

was operated at 400 MHz at room temperature. The chromatographic separation of the analytes was achieved with an LC-10A high-performance liquid chromatograph (Shimadzu Corporation, Japan). Thermogravimetric analysis was carried out using a PerkinElmer Pyris 1 TGA instrument. The samples were heated at a constant rate of 10  $^{\circ}\text{C}/\text{min}$  under nitrogen atmosphere.

N,N-dimethylformamide, sodium hydroxide, hydrochloric acid, potassium iodide, carbinol, methanol, acetonitrile, acetone, 1,2-dimethyl imidazole (Shanghai Chemical Reagent Corporation, China),  $\beta$ -CD (Xi'an Hongchang Pharmaceutical Corporation, China), and hexamethylene diisocyanate (Aladdin Reagent Corporation, Shanghai, China) were used in the experiment. The stock solution of 100.0  $\mu\text{g}/\text{mL}$  magnolol was prepared by being directly dissolved in ethanol and kept in the dark all the time.

### 2.2. Synthesis of ILs- $\beta$ -CDCP

The synthesis procedure for ILs- $\beta$ -CDCP is depicted in Fig. 2. The intermediates  $\beta$ -CDOTs(a),  $\beta$ -CDI(b) and ILs- $\beta$ -CD(c) were prepared according to the literature [21,22,33]. ILs- $\beta$ -CD(d) (2.08 mmol) was dissolved in DMF (30 mL) and hexamethylene diisocyanate (HDI, 12.5 mmol) mixed with 10 mL DMF was added by drops. The reaction mixture was heated to 75  $^{\circ}\text{C}$  and stirred for 24 h at this temperature. After being cooled to room temperature, the obtained sticky liquid was treated with acetone to produce white solid. The acetone was removed by filtration. The white solid was dried in vacuum oven at 50  $^{\circ}\text{C}$  for 12 h and then ground into powder.  $\beta$ -CDCP was synthesized in the same way.

### 2.3. Determination method

At room temperature, the sample solution after treatment and the pH buffer were added into a tube, and then distilled water was added to 50 mL. 0.1 g ILs- $\beta$ -CDCP was added into the tube. The mixture was shaken on the timing multifunctional oscillator for 16.0 min and then centrifuged. Methanol of 5.0 mL as elution was added into the used ILs- $\beta$ -CDCP. The mixture was ultrasonically vibrated at room temperature for 20 min and then centrifuged to obtain a supernatant solution. The supernatant solution was determined with HPLC.

### 2.4. Sample preparation

The drug membrane was removed. A drug sample of 1.25 g was dissolved in 25 mL methanol, ultrasonically extracted for 30 min and then filtrated to obtain a supernatant. The solution was transferred into a 25 mL volumetric flask and diluted to the mark with methanol.

### 2.5. Chromatographic condition

Separations were obtained on a C18 reversed-phase column (250 mm  $\times$  4.6 mm I.D., 5  $\mu\text{m}$ , Shimadzu Corporation, Japan) kept at 25  $^{\circ}\text{C}$ . The injection was carried out through a 20  $\mu\text{L}$  loop. A mixed solution of methanol and water at the volume ratio of 75:25 was used as the mobile phase in HPLC. The flow rate was 1 mL/min and the UV/vis detector was set at 294 nm for all samples.

### 2.6. Determination of inclusion constant

The procedure of determination of inclusion constant was based on the literature [34].

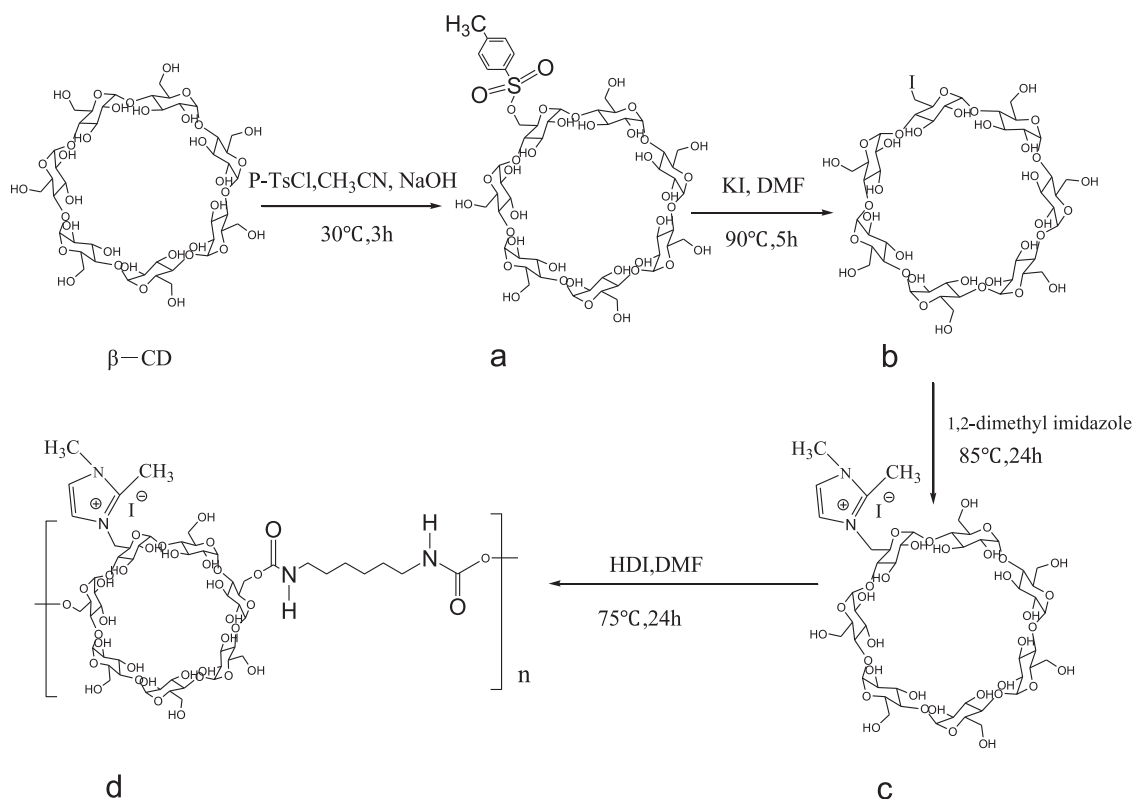


**Fig. 2** Synthesis scheme of ILs-β-CDCP. (a) β-CDOTs, (b) β-CDI, (c) ILs-β-CD and (d) ILs-β-CDCP.

### 3. Results and discussion

#### 3.1. Characterization of ILs-β-CDCP

In this work, ionic liquids functionalized β-cyclodextrin polymer (ILs-β-CDCP) was characterized by FTIR, <sup>1</sup>H nuclear magnetic resonance (NMR), and <sup>13</sup>C CP/MAS NMR.

##### 3.1.1. Characterization by FTIR

The FTIR spectra of ILs-β-CD (curve a) and ILs-β-CDCP (curve b) are shown in Fig. 3. Characterization data are as follows:

- ILs-β-CD (IR/KBr, cm<sup>-1</sup>) 3703, 3308, 2929, 1720, 1027, 1586, 1411, 1156, 1034. The peaks of 1156 cm<sup>-1</sup> corresponded to σC–N vibration. It confirmed the synthesis of monomer ILs-β-CD.
- ILs-β-CDCP (IR/KBr, cm<sup>-1</sup>) 3373, 2932, 2860, 1713, 1660, 1556, 1259, 1031. The peaks of 2932, 2860 cm<sup>-1</sup> corresponded to ν<sub>as</sub> and ν<sub>s</sub> vibration of methylenes which were the characteristic groups of hexamethylene diisocyanate. The peaks of 1660, 1566, and 1259 cm<sup>-1</sup> corresponded to the absorption bands I, II and III of amide, which confirmed the formation of ionic liquids functionalized β-cyclodextrin polymer ILs-β-CDCP.

##### 3.1.2. Characterization by <sup>1</sup>H NMR

<sup>1</sup>H NMR characterization data of ionic liquids functionalized β-cyclodextrin polymer are as follows:

ILs-β-CD (<sup>1</sup>H NMR/ppm, 600 MHz, DMSO-d<sub>6</sub>): 7.6 (d, H<sub>Ar</sub>), 5.64–5.80 (m, OH-2, OH-3), 4.45–4.83 (m, H-1), 4.32–4.51 (m, OH-6), 3.71 (s, –CH<sub>3</sub>), 3.41–3.67 (m, H-2, H-3, H-4, H-5, H-6),

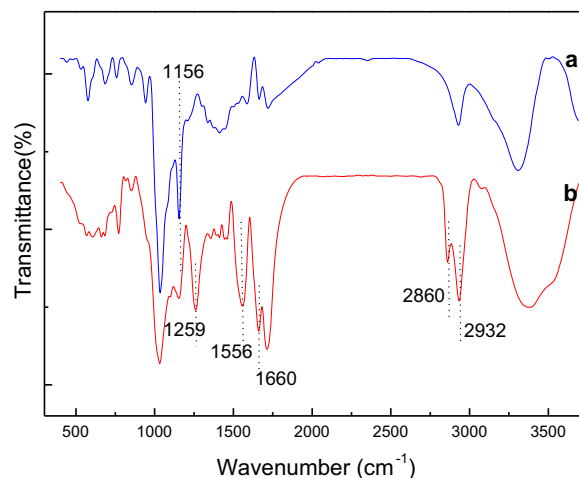


**Fig. 3** FTIR spectra of (a) ILs-β-CD and (b) ILs-β-CDCP.

and 2.68 (s, –CH<sub>3</sub>). It indicated that ionic liquids functionalized β-cyclodextrin polymer was ILs-β-CD.

##### 3.1.3. Characterization by <sup>13</sup>C CP/MAS NMR

Fig. 4 shows the <sup>13</sup>C CP/MAS NMR spectra of β-CDCP (curve a) and ILs-β-CDCP (curve b).

The spectra of β-CDCP and ILs-β-CDCP were similar because they both had β-cyclodextrin as the main body, but there were still some differences between them. (1) ILs-β-CDCP (curve b) had the characteristic peaks at 143.9, 123.3 and 122.0 ppm which respectively, corresponded to the chemical shifts of no.2',4',5' carbons of 1,2-dimethyl imidazole, thus confirming the formation of ILs-β-CDCP. (2) Both β-CDCP (curve a) and ILs-β-CDCP (curve b) had

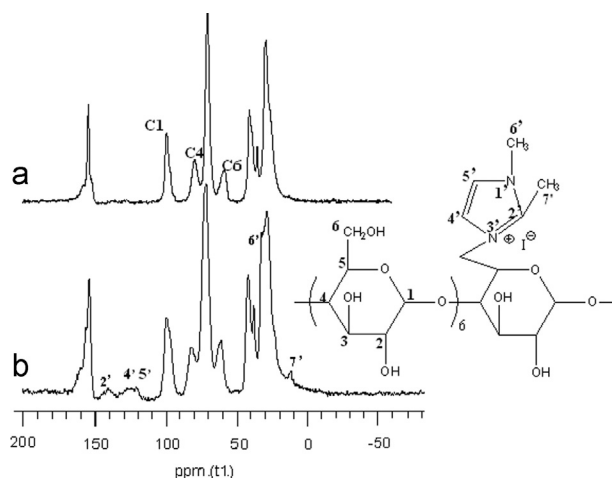


**Fig. 4**  $^{13}\text{C}$  CP/MAS NMR spectra of (a)  $\beta$ -CD-CP and (b) ILs- $\beta$ -CD-CP.

chemical shifts at 102.7, 83.4 and 59.9 ppm which were chemical shifts for no. 1,4,6 carbons of pyranose in the main body of  $\beta$ -cyclodextrin. The spectra of ILs- $\beta$ -CD-CP (curve b) showed that the split of the chemical shifts at 81.7 and 51.3 ppm declined due to the modification of  $\beta$ -cyclodextrin matrix. All these confirmed the formation of ionic liquids functionalized  $\beta$ -cyclodextrin polymer ILs- $\beta$ -CD-CP.

### 3.2. Optimization of adsorption

The factors affecting the adsorption process of magnolol such as pH, temperature and solution volume were studied. Adsorption behavior of ILs- $\beta$ -CD-CP was compared with that of  $\beta$ -CD-CP.

#### 3.2.1. Effect of pH

As shown in Fig. 5, (1) adsorption efficiency of magnolol on ILs- $\beta$ -CD-CP (curve 1) was always higher than that on  $\beta$ -CD-CP (curve 2), although their tendency was almost the same; (2) the adsorption efficiency of magnolol on ILs- $\beta$ -CD-CP was above 90.0% when the pH was in the range of 7.0–13.0 and lower than 6.0. It reached the highest value of 97.6% when pH was 12.0. Magnolol is electrically negative in strong alkaline (the dissociation constants of magnolol  $\text{pK}_{\text{a}1}$  and  $\text{pK}_{\text{a}2}$  are about 7.10 and 10.58 [35]). So, adsorption efficiency of magnolol on ILs- $\beta$ -CD-CP was higher than that on  $\beta$ -CD-CP due to the electrostatic attraction between the cation of ionic liquid and the electrically negative magnolol.

#### 3.2.2. Effect of adsorption temperature

The adsorption efficiency of magnolol on ILs- $\beta$ -CD-CP (curve 1) and  $\beta$ -CD-CP (curve 2) at different temperatures (0.0–60.0 °C) was studied (Fig. 6). The adsorption efficiency of magnolol on ILs- $\beta$ -CD-CP was higher than that on  $\beta$ -CD-CP and was above 90% from 0.0 °C to 60.0 °C. The experiment was carried out at room temperature.

#### 3.2.3. Effect of the sample volume

The amount of magnolol was fixed at 20.0  $\mu\text{g}$  and the volume of the sample solution increased from 5.0 mL to 70.0 mL. The adsorption efficiency was above 85% at sample volume of

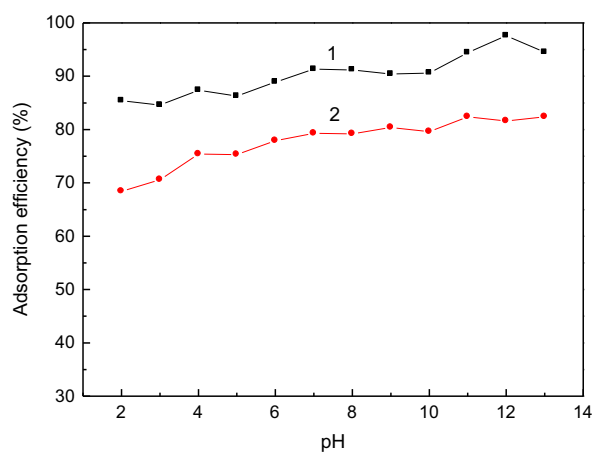


**Fig. 5** Effect of pH on adsorption efficiency ( $c_0=2.00 \mu\text{g/mL}$ ) (curve 1: ILs- $\beta$ -CD-CP, curve 2:  $\beta$ -CD-CP).

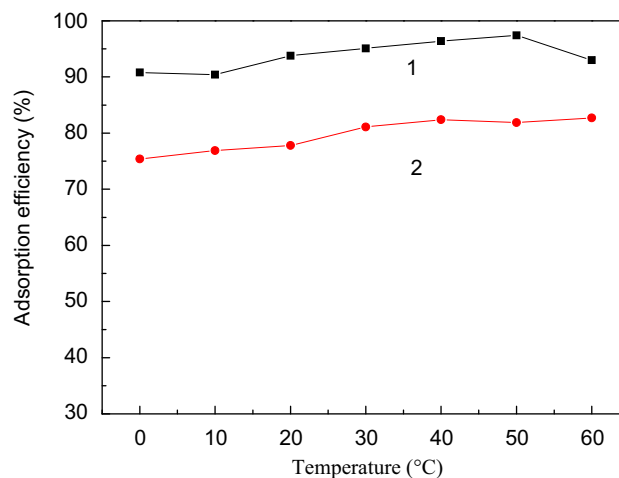


**Fig. 6** Effect of temperature on adsorption efficiency ( $c_0=2.00 \mu\text{g/mL}$ ) (curve 1: ILs- $\beta$ -CD-CP, curve 2:  $\beta$ -CD-CP).

60.0 mL and decreased to 80.3% when the sample volume was 70.0 mL. So the largest sample volume allowed was 60.0 mL.

### 3.3. Adsorption kinetics

The adsorption process was completed within 16.0 min, and the adsorption efficiency remained almost stable (94.0%). 16.0 min as the adsorption time for magnolol was adopted.

### 3.4. Adsorption capacity

The adsorption capacity is defined as the maximum amount of magnolol adsorbed per gram of the polymer. The adsorption capacity of magnolol for ILs- $\beta$ -CD-CP (curve 1) and  $\beta$ -CD-CP (curve 2) was studied (Fig. 7). The adsorption of magnolol on ILs- $\beta$ -CD-CP reached the maximum value when the concentration of magnolol was 12.0  $\mu\text{g/mL}$ . The adsorption capacity for ILs- $\beta$ -CD-CP was calculated as 3.64 mg/g while that on  $\beta$ -CD-CP (2.36 mg/g) was smaller.

### 3.5. Optimization of elution

Different eluents were investigated (Fig. 8). The order of elution efficiency was methanol (93.4%) > ethanol (91.5%) > SDS (63.4%) > ethyl acetate (54.6%) > HCl (10.7%). So methanol was adopted as the eluent.

Elution efficiency of magnolol with 3.5–8.0 mL of methanol was studied. The elution efficiency of magnolol was above 92% from 5.0 to 8.0 mL. The preconcentration factor was 12 (the quotient of volume before absorption and after elution). And

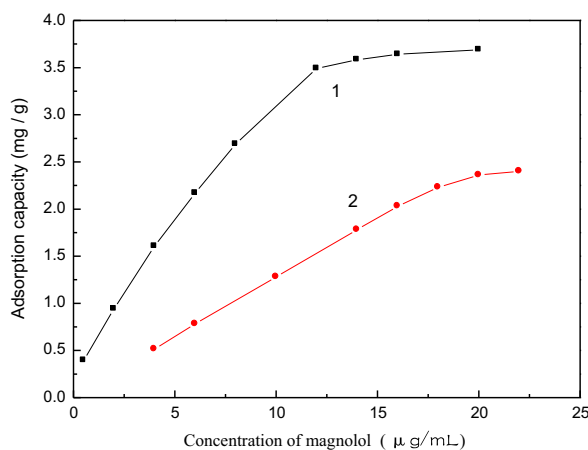


Fig. 7 Adsorption capacity (curve 1: ILs-β-CDPC, curve 2: β-CDPC).

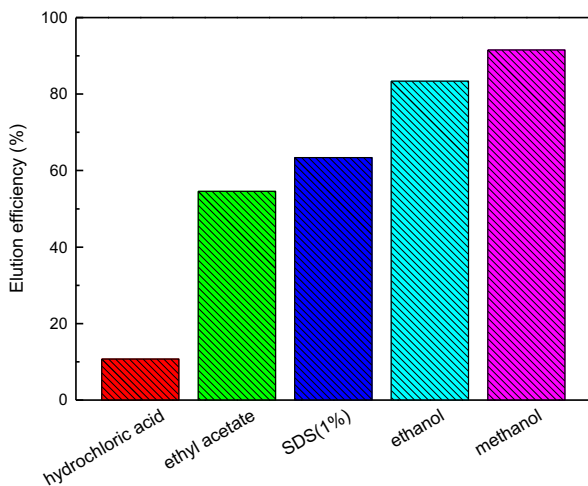


Fig. 8 Effect of different dissolvents on elution efficiency.

the optimum volume of methanol chosen for this work was 5.0 mL.

The elution process was completed within 20.0 min, and the elution efficiency did not change with a stable elution efficiency of 95.0% thereafter. The elution time of 20.0 min for magnolol was adopted.

### 3.6. Effect of interferences

With a relative error less than  $\pm 5\%$ , the influence of some interferences that drug samples contained on the determination of magnolol was studied and the tolerance limit is shown in Table 1. The results indicated that the majority of these substances in the samples had no remarkable interference on the magnolol determination. The 12-fold honokiol (as an isomer) did not affect its determination, either. It should be noted that the contents of honokiol in real samples were of very low levels, which did not affect the analysis of magnolol.

### 3.7. Analytical performance of the method

Under optimum conditions described above, ILs-β-CDPC showed a linear calibration curve within the concentration range of 0.02–8.00 μg/mL. The equations of calibration graph was I (peak area) = 185.58 + 2288.514c (μg/mL) with a correlation coefficient of 0.9992. The limit of detection (LOD) was 1.9 ng/mL. The relative standard deviation was 2.76% ( $n=3$ ,  $c=2.0$  μg/mL). The enhancement factor, defined as the quotient of volume before absorption and after elution, was 12.

### 3.8. Determination of magnolol in drug samples

Fig. 9 shows the chromatographic peak of magnolol standard solution before and after extraction (curve a, curve b), magnolol in drug sample of Huoxiang Zhengqi capsule before and after extraction (curve c, curve d). It indicated that the retention time of magnolol was 8.65 min (curve a, curve b) and that the concentration of magnolol increased significantly after preconcentration (curve c, curve d).

The proposed method was applied to determine the amount of magnolol in drug samples compared with HPLC method (Table 2). The statistical  $t$ -test ( $P=0.95$ ) was used to compare the results from both methods, which showed no significant difference between them.

### 3.9. Comparison with other methods

Various methods for detection of magnolol have been reported: electrochemical method, fluorescent spectrometry, and high-perfor-

Table 1 Tolerance of interferences on the determination of magnolol (tolerance ratio in mass).

Interferent	Tolerance ratio	Interferent	Tolerance ratio
Ca <sup>2+</sup> , Cu <sup>2+</sup>	200	Ursolic acid	25
Zn <sup>2+</sup> , Mg <sup>2+</sup> , Na <sup>+</sup> , K <sup>+</sup>	500	Geniposide	20
Glucose	500	Baicalin	10
Sodium citrate	100	Honokiol	12

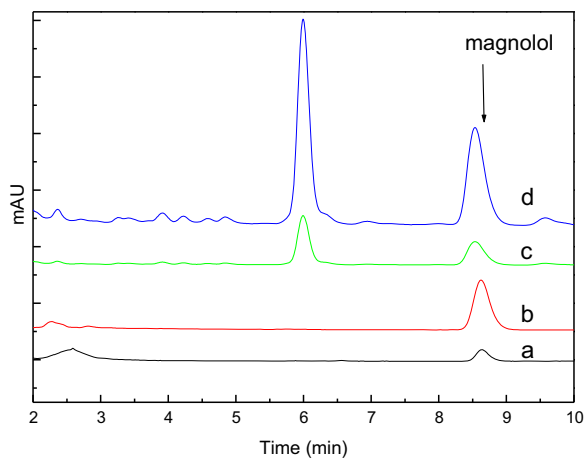


**Fig. 9** The chromatographic peak of (a) magnolol standard solution before extraction; (b) magnolol standard solution after extraction; (c) drug sample before extraction and (d) drug sample after extraction.

mance liquid chromatography [36,37]. Compared with other reported methods, the method adopted in the present work obviously had a higher sensitivity and a wider linear range (Table 3).

### 3.10. The adsorption mechanism of ILS- $\beta$ -CDCP

Discussion of adsorption mechanism mainly included the inclusion effect (as the dominant role) of the cyclodextrin cavity (ILS- $\beta$ -CDCP) and magnolol and electrostatic attraction effect (as discussed in Section 3.2.1). The inclusion effect of ILS- $\beta$ -CDCP and magnolol was studied through the calculation of inclusion constant, FTIR and TGA analysis.

#### 3.10.1. Inclusion constant

The inclusion constant  $K$  is a significant parameter which presents inclusion properties of host-guest molecules. The inclusion complex can be easily formed at a higher  $K$ . The inclusion constant was calculated according to Benesi-Hildebrand equation (double reciprocal plot) [34]. In this paper, the inclusion constants of the

**Table 2** Magnolol in drug samples ( $n=3$ ).

Sample	Proposed method <sup>a</sup> (mg/g)	HPLC method (mg/g)
Huoxiang Zhengqi capsule	0.8645	0.8934
Huoxiang Zhengqi pill	0.3427	0.3618
Weilikang tablet	0.2889	0.3046

<sup>a</sup>The sample solution was diluted 10 times before detection.

**Table 3** Comparison with the results in the literature.

Method	LOD	Linear range	Ref.
Second order derivative synchronous fluorimetry	0.84 $\mu\text{g/L}$	2.8–500 $\mu\text{g/L}$	[28]
Micelle-stabilized fluorimetry	0.002 mg/L	0.2–6 mg/L	[30]
Voltammetry	$2.5 \times 10^{-8}$ M	$7.5 \times 10^{-8}$ – $2.0 \times 10^{-5}$ $\mu\text{g/mL}$	[36]
HPLC	25 ng/mL	40–400 ng/mL	[37]
SPE-HPLC	1.9 ng/mL	0.02–8 $\mu\text{g/mL}$	The proposed method

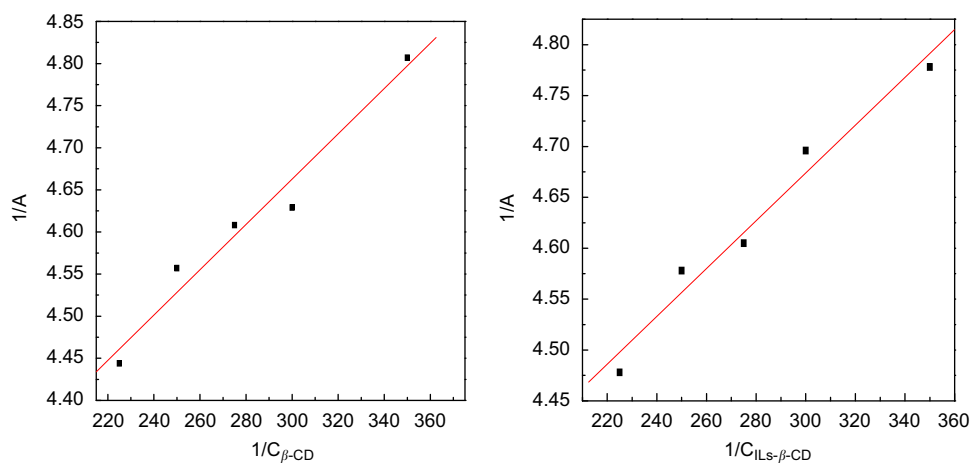


**Fig. 10** Double reciprocal plot of  $\beta$ -CD–magnolol inclusion complex and ILS- $\beta$ -CD–magnolol inclusion complex.

monomers of two kinds of polymers ( $\beta$ -CD and ILS- $\beta$ -CD) and magnolol were obtained.

The double reciprocal plots of the  $\beta$ -CD–magnolol inclusion complex and ILS- $\beta$ -CD–magnolol inclusion complex are shown in Fig. 10. The two double reciprocal plots showed a good linearity with correlation coefficients of 0.9818 for  $\beta$ -CD and 0.9845 for ILS- $\beta$ -CD. It could be concluded that both  $\beta$ -CD and ILS- $\beta$ -CD form the inclusion complexes with magnolol at the ratio of 1:1. The inclusion constant ( $K$ ) of ILS- $\beta$ -CD–magnolol inclusion complex was  $1.433 \times 10^3$  L/mol, which was higher than  $1.689 \times 10^3$  L/mol for  $\beta$ -CD–magnolol. It indicated that the inclusion ability of ILS- $\beta$ -CD toward magnolol was stronger than that of

$\beta$ -CD. It was one reason why adsorption efficiency of ILS- $\beta$ -CDCP was better than that of  $\beta$ -CDCP.

### 3.10.2. FTIR analysis

Fig. 11 shows the FTIR spectra of ILS- $\beta$ -CDCP (curve a), ILS- $\beta$ -CDCP–magnolol inclusion complex (curve b), and magnolol (curve c). It indicated that (1) the peak at  $1638\text{ cm}^{-1}$ , which corresponded to the  $\nu\text{C}=\text{C}$  vibration of magnolol, appeared in the spectra of ILS- $\beta$ -CDCP–magnolol inclusion complex. It confirmed the formation of ILS- $\beta$ -CDCP–magnolol inclusion complex (curves a, b); (2) the peaks at  $3157\text{ cm}^{-1}$  and  $908\text{ cm}^{-1}$  were the stretching vibration of C–H ( $\nu\text{C-H}$ ) and the bending vibration of C–H ( $\delta\text{C-H}$ ) in benzene ring of magnolol. The peak at  $1497\text{ cm}^{-1}$  corresponded to the skeletal vibration of benzene ring in magnolol (curve c). The above characteristic peaks disappeared in the spectra of ILS- $\beta$ -CDCP–magnolol, which illustrated the aromatic ring of magnolol was included in the hydrophobic cavity of ILS- $\beta$ -CDCP.

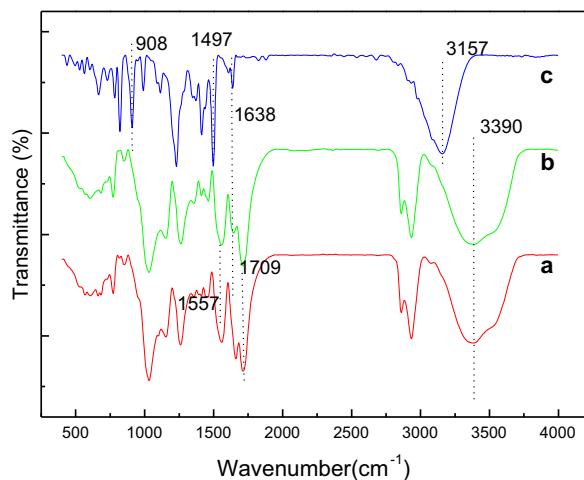


Fig. 11 FTIR spectra of (a) ILS- $\beta$ -CDCP, (b) ILS- $\beta$ -CDCP–magnolol inclusion complex and (c) magnolol.

### 3.10.3. TGA analysis

The TGA spectra of ILS- $\beta$ -CDCP (curve a), ILS- $\beta$ -CDCP–magnolol inclusion complex (curve b) and the mixture of ILS- $\beta$ -CDCP and magnolol (curve c) are shown in Fig. 12. Their decomposition temperature and the loss of weight percentage are shown in Table 4. Two points can be concluded: (1) the temperature of initial decomposition of ILS- $\beta$ -CDCP–magnolol inclusion complex (curve b) was lower than that of ILS- $\beta$ -CDCP (curve a), because the guest molecule magnolol included in the inclusion complex began to decompose; (2) compared with ILS- $\beta$ -CDCP–magnolol inclusion complex (curve b), the initial decomposition temperature of the mixture of ILS- $\beta$ -CDCP and magnolol (curve c) was lower and at the first decomposition stage the mixture had a higher percentage of weight loss. It was observed that the formation of inclusion complex delayed the weight loss of the guest molecule (magnolol). That is to say, the thermal stability of guest (magnolol) molecule was improved when ILS- $\beta$ -CDCP was included.

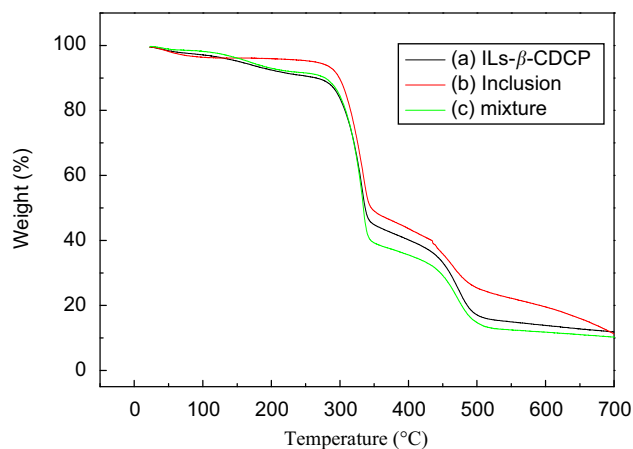


Fig. 12 TGA spectra of (a) ILS- $\beta$ -CDCP, (b) ILS- $\beta$ -CDCP–magnolol inclusion complex and (c) ILS- $\beta$ -CDCP+magnolol.

## 4. Conclusion

In this work, ILS- $\beta$ -CDCP was synthesized as a solid-phase extraction material to pre-concentrate/separate magnolol coupled with HPLC for the analysis of magnolol. Compared with  $\beta$ -CDCP, ILS- $\beta$ -CDCP showed a better adsorption capacity. The proposed method for the analysis of magnolol was satisfactory.

## Acknowledgments

The authors acknowledge the financial support from the National Natural Science Foundation of China (Nos. 21155001 and 21375117) and a project funded by the Priority Academic Program

Table 4 The decomposition temperature and weight loss.

System	Decomposition temperature 1 (°C)	Decomposition temperature 2 (°C)	Weight loss in first stage (%)	Weight loss in second stage (%)
ILS- $\beta$ -CDCP	90.98	381.26	55.52	30.03
Inclusion complex	88.28	386.86	51.14	33.73
Physical mixture	80.43	380.68	58.51	26.69

Development of Jiangsu Higher Education Institutions, and the Foundation of the Excellence Science and Technology Invention Team in Yangzhou University.

## References

- [1] M.C. Hennion, Solid-phase extraction: method development, sorbent, and coupling with liquid chromatography, *J. Chromatogr. A* 856 (1-2) (1999) 3–54.
- [2] M. Vukcevic, A. Kalijadis, M. Radisic, et al., Application of carbonized hemp fibers as a new solid-phase extraction sorbent for analysis of pesticides in water samples, *Chem. Eng. J.* 211–212 (2012) 224–232.
- [3] D. Panavaite, A. Padaruskas, V. Vickackaite, Silicone glue coated stainless steel wire for solid phase microextraction, *Anal. Chim. Acta* 571 (1) (2006) 45–50.
- [4] S. Kagaya, E. Maeba, Y. Inoue, et al., A solid phase extraction using a chelate resin immobilizing carboxymethylated pentaethylenhexamine for separation and preconcentration of trace elements in water samples, *Talanta* 79 (2) (2009) 146–152.
- [5] H. Abdolmohammad-Zadeh, Z. Rezvani, G.H. Sadeghi, et al., Layered double hydroxides: a novel nano-sorbent for solid-phase extraction, *Anal. Chim. Acta* 685 (2) (2011) 212–219.
- [6] M. Ghaedi, F. Ahmadi, Z. Tavakoli, et al., Three modified activated carbons by different ligands for the solid phase extraction of copper and lead, *J. Hazard. Mater.* 152 (3) (2008) 1248–1255.
- [7] X.S. Zhu, M. Wu, Y. Gu,  $\beta$ -cyclodextrin-cross-linked polymer as solid phase extraction material coupled with inductively coupled plasma mass spectrometry for the analysis of trace Co(II), *Talanta* 78 (2) (2009) 565–569.
- [8] Y. Che, Y. Gu, X.S. Zhu, Enriching cadmium by inclusion absorbing resin with  $\beta$ -cyclodextrin cross-linking polymer, *J. Yangzhou Univ. (Nat. Sci. Edit.)* 12 (3) (2009) 26–29.
- [9] X.Q. Yang, H.O. Qiu, J.L. Li, et al., Determination of platinum in geological samples by graphite furnace atomic absorption spectrometry after enrichment with  $\beta$ -cyclodextrin cross-linking polymer, *Chin. J. Anal. Chem.* 33 (9) (2005) 1275–1278.
- [10] Y.J. Li, Enriching copper by inclusion absorbing resin with  $\beta$ -cyclodextrin cross-linking polymer, *Chin. J. Anal. Lab.* 23 (3) (2004) 53–55.
- [11] M. Wu, X.S. Zhu,  $\beta$ -Cyclodextrin-cross-linked polymer coupled ultraviolet-visible spectrophotometry for separation and analysis of p-nitrophenol, *Chin. J. Anal. Chem.* 37 (11) (2009) 1691–1694.
- [12] D.L. Zou, S.Y. Tang, H.F. Xiong, et al., Adsorption characteristic of chlorobenzene in water by  $\beta$ -cyclodextrin-cross-linked polymer, *J. Jilin Univ.* 42 (4) (2012) 1166–1172.
- [13] J. Szejtli, Introduction and general overview of cyclodextrin chemistry, *Chem. Rev.* 98 (5) (1998) 1743–1753.
- [14] K.G. Chai, H.B. Ji, Dual functional adsorption of benzoic acid from wastewater by biological-based chitosan grafted  $\beta$ -cyclodextrin, *Chem. Eng. J.* 203 (2012) 309–318.
- [15] A.Z.M. Badruddoza, A.S.H. Tay, P.Y. Tan, et al., Carboxymethyl- $\beta$ -cyclodextrin conjugated magnetic nanoparticles as nano-adsorbents for removal of copper ions: synthesis and adsorption studies, *J. Hazard. Mater.* 185 (2–3) (2011) 1177–1186.
- [16] H.X. Wang, Y.H. Zhou, Y.J. Guo, et al.,  $\beta$ -Cyclodextrin/Fe<sub>3</sub>O<sub>4</sub> hybrid magnetic nano-composite modified glassy carbon electrode for tryptophan sensing, *Sens. Actuators B* 163 (1) (2012) 171–178.
- [17] J.L. Anderson, J. Ding, T. Welton, et al., Characterizing ionic liquids on the basis of multiple solvation interactions, *J. Am. Chem. Soc.* 124 (47) (2002) 14247–14254.
- [18] S. Keskin, D.K. Talay, U. Akman, et al., A review of ionic liquids towards supercritical fluid applications, *J. Supercrit. Fluids* 43 (1) (2007) 150–180.
- [19] C.D. Tran, S.H.D.P. Lacerda, Determination of binding constants of cyclodextrins in room-temperature ionic liquids by near-infrared spectrometry, *Anal. Chem.* 74 (2002) 5337–5341.
- [20] N. Li, J. Liu, X.Y. Zhao, et al., Complex formation of ionic liquid surfactant and  $\beta$ -cyclodextrin, *Colloid Surf. A* 292 (2007) 196–201.
- [21] Z.M. Zhou, X. Li, X.P. Chen, et al., Synthesis of ionic liquids functionalized  $\beta$ -cyclodextrin-bonded chiral stationary phases and their applications in high-performance liquid chromatography, *Anal. Chim. Acta* 678 (2) (2010) 208–214.
- [22] M.M. Mahlambi, T.J. Malefetse, B.B. Mamba, et al.,  $\beta$ -Cyclodextrin-ionic liquid polyurethanes for the removal of organic pollutants and heavy metals from water: synthesis and characterization, *J. Polym. Res.* 17 (4) (2010) 589–600.
- [23] H.M. Wang, S.W. Zhang, The research progress in pharmacological effects of magnolol, *Beijing J. Tradit. Chin. Med.* 28 (7) (2009) 562–565.
- [24] C.L. Chen, P.L. Chang, S.S. Lee, et al., Analysis of magnolol and honokiol in biological fluids by capillary zone electrophoresis, *J. Chromatogr. A* 1142 (2) (2007) 240–244.
- [25] X.L. Zhang, Determination of patchouli alcohol honokiol in Jiawei-huoxiangzhengqi pills (Houxiangzhengqi pills) by gas chromatography, *Chin. Pharm.* 11 (1) (2008) 46–47.
- [26] H. Li, B.K. Zhang, Y.G. Zhu, et al., Assay of zinc in pharmacutis by atomic absorption spectrophotometry, *Chin. J. Pharm. Anal.* 18 (3) (1998) 182–185.
- [27] X.Y. Wang, X.H. Bai, H.F. Zhang, et al., Determination of magnolol and honokiol in rats by liquid-phase microextraction with nonaqueous back extraction coupled with HPLC, *Chin. Hosp. Pharm.* 28 (10) (2008) 780–784.
- [28] J. Yang, D.S. Yu, S.P. Liu, et al., Simultaneous direct determination of magnolol and honokiol by second order derivative synchronous fluorimetry, *Chin. J. Anal. Chem.* 37 (1) (2009) 107–110.
- [29] L. Pang, G.H. Chen, Y.L. Tiang, et al., Determination of magnolol and honokiol in the herb of magnolia of ficinal is by fluorescence spectrophotometry, *J. Hebei Univ.* 24 (2) (2004) 159–162.
- [30] X.H. Bai, Y.S. Wei, C.S. Liu, Simultaneous determination of magnolol and honokiol by micelle-stabilized fluorimetry, *Chin. J. Anal. Chem.* 27 (4) (1999) 388–391.
- [31] Z.J. Bao, X.Q. Yang, Z.T. Ding, et al., Simultaneous determination of magnolol and honokiol by UV spectrophotometry free radical scavenger activity, *Nut. Prod. Res. Dev.* 16 (5) (2004) 435–438.
- [32] X. Yu, F. Feng, B. Teng, et al., Dispersive liquid-liquid microextraction-HPLC for the determination of magnolol and honokiol in huoxiangzhengqi oral solution, *Pharm. Clin. Res.* 20 (3) (2012) 264–266.
- [33] N. Zhong, H.S. Byun, R. Bittman, An improved synthesis of 6-O-monotosyl-6-deoxy- $\beta$ -cyclodextrin, *Tetrahedron Lett.* 39 (19) (1998) 2919–2920.
- [34] K. Wan, T.F. Li, Q. Lu, et al., Effect of the pH on the  $\beta$ -cyclodextrins inclusion complex with methylene blue, *Chem. Res. Appl.* 18 (8) (2006) 917–920.
- [35] Z.J. Bao, L. Dai, Z.T. Miao, et al., Determination of the dissociation constants of magnolol and honokiol by UV spectrophotometry, *J. Yunnan Univ. (Nat. Sci. Edit.)* 26 (1) (2004) 66–69.
- [36] T. Liu, X.J. Zheng, W.S. Huang, et al., Voltammetric detection of magnolol in Chinese medicine based on the enhancement effect of mesoporous Al/SiO<sub>2</sub>-modified electrode, *Colloid Surf. B* 65 (2) (2008) 226–229.
- [37] X. Wu, X. Chen, Z. Hu, High-performance liquid chromatographic method for simultaneous determination of honokiol and magnolol in rat plasma, *Talanta* 59 (1) (2003) 115–121.